The Pennsylvania State University

The Graduate School

MINIMIZING THE COST FOR CHARGING PLUG-IN ELECTRIC VEHICLES USING BFGS QUASI-NEWTON METHOD

A Thesis in

Electrical Engineering

by
Zhiran Li

Submitted in Partial Fulfillment
of the Requirements
for the Degree of

Master of Science

August 2022

The thesis of Zhiran Li was reviewed and approved by the following:

Yan Li
Professor of Electrical Engineering
Thesis Advisor

Donald E Ebeigbe
Professor of Electrical Engineering
Committee Member

Kultegin Aydin
Head of the Department of Electrical Engineering
Professor of Electrical Engineering

Abstract

This thesis presents a Broyden–Fletcher–Goldfarb–Shanno (BFGS)-enabled Quasi-Newton method to minimize the cost for charging Plug-in Electric Vehicles (PEVs). Firstly, the objective function for minimizing the cost for charging PEVs is introduced, as well as the constraints on the charger, the state of charge, and the voltage levels. Secondly, the mathematical formulas of the BFGS Quasi-Newton algorithm are presented to calculate the voltage of a node topology. After that, the charging results for using both Newton's method and BFGS Quasi-Newton method are compared in two scenario cases. The grid system in the first scenario is a traditional power grid that consists of 18 power nodes. And the power node is a PEV charging station that can handle bidirectional power flow. And the grid system in the second grid topology is a micro-grid system that consists of 8 power nodes and 10 Distributed Energy Resources (DER) generation buses including photovoltaic, micro-turbine and fuel cell etc. The test result also shows BFGS-enabled method has a lower cost in charging PEVs than using the Newton's method in same grid topology and same situation. Therefore, the comparison between the BFGS-enabled Quasi-Newton method and Newton's method verifies that the BFGS-enabled method can better minimize the cost for charging PEVs.

Index Terms: Minimizing the cost of charging, Optimization methods, Quasi-Newton method, Newton's method, Broyden–Fletcher–Goldfarb–Shanno (BFGS), Plug-in Electric Vehicles (PEVs).

Contents

List of Figures

List of Tables

Acknowledgements

I would like to thank my advisor, Dr. Yan Li, for supervising this thesis. She guided me very well.

Special thanks to the authors Ovalle Villamil, Andres & Hably, Ahmad & Seddik, Bacha in (1), the centralized approach. Their paper inspired me a lot. And the MATLAB code they provided gave me a solid fundamental to my thesis.

Thanks to my friend Zhihan Liu, who taught me and gave me suggestion to use BFGS Quasi-Newton method in my thesis.

Thanks to my friend Jinkai Yang, who taught me in using MATLAB to calculate the base voltage for the grid topology.

1 Introduction

Plug-in Electric Vehicles (PEVs) have a battery instead of a gasoline tank, and an electric motor instead of an internal combustion engine. PEVs can be charged from the electric grid, and the electricity stored in the rechargeable battery pack. But the charging price for PEVs is not cheap. According to John Voelcker, a long time automotive journalist and industry analyst who specializes in electric vehicles, that a PEV gets three to four miles per kilowatt hour (kWh). So, the electrical energy used in charging a PEV can be estimated by dividing the total miles by three (or four). Then we can estimate the charging price by multiplying the number by the price per kWh. According to the statistical study, Americans drive an average of 14,200 miles annually, that is 1,183 miles per month (2). And that means 394 kWh electricity is used in charging the PEV per month. The U.S. household electricity price in January 2022 is nearly 14 cents per kWh. Charging a PEV can cost around 55 dollars per month (3). Reducing the 55 dollars charging cost as much as possible is beneficial. Therefore, it is necessary to minimize the cost of charging PEVs. Electricity rates are subjected to many factors, including the region where people live, the time of year, and even the time of day when peak charges apply. For the most part, electricity usage and costs are at their lowest late at night. During 11 PM to 6 AM, the electricity tariff is lower than the time during high tariff hour. Normally, it can be observed that the peak consumption of household electricity usage is at 6 PM. it is then reduced and increased again to the peak of consumption at 8 AM. That is good news for anyone considering a PEV, according to Voelcker. The cheapest way to charge electric car is almost always at home, overnight. Some utilities have special low rates for the overnight period when their demand is lightest. However, the price for installing a level 2 charger in the garage is very high which can cost a large amount of money. According to the data from home guide, installing a level 2 charging station, a 240V outlet, wiring, and wall mounting at home costs around 2,000 dollars (4). And a Tesla wall connector charger costs 500 dollars and the installation fee is around 800 to 1,000 dollars average. Therefore, it costs a lot to install the charger at home though it is the cheapest way to charge electric cars.

The problem discussed in this thesis is to consider the situation of charging the PEVs at charging stations instead of at home chargers. The goal is to use a proper optimization method to minimize the cost of charging several PEVs at charging stations. For example, let us assume there are three PEVs starting to charge at 18 PM with different states of charge remaining in their battery. PEV1 has an initial state of charge of 40%, PEV2 has an initial state of charge of 20%, and PEV 3 has an initial state of charge of 50%, respectively. All the three PEVs use the same capacity battery of 16 kWh. And their desired state of charge is to fully charge their battery. Without any charging management, the chargers are using the maximum charging rates to charge the batteries.The chargers are all assumed to have a maximum charging rates of 3 kW. So it will use 3.2 hours to charge the first PEV, 4.27 hours for the second PEV, and 2.67 hours for the third PEV (1). This situation does not consider selling the electricity back to the charger at the high tariff hour, thus not the result we desired. Therefore, in order to get the minimize cost of charging, an optimization method has to be applied into this scenario, and constraints needed to be set for charging rates, voltage levels, maximum state of charge, etc. There are several optimization methods. For example, Newton's method and Gradient descent method.

Previous papers and research used several different optimization methods to optimize the cost for charging PEVs. Firstly, Dr. Ovalle et al. used Newton's method in chapter 2 of the book *Grid Optimal Integration of Electric Vehicles: Examples with Matlab Implementation* to optimize the cost of charging schedules for PEVs. The proposed approach in this chapter considers PEV charging integration in different situations, and this chapter takes into account the constraints on voltage of chargers, the limits on the state of charge, and the voltage levels at the different nodes of the grid (1). In order to integrate these constraints in the objective function, an approximated linear model for low voltage distribution systems is employed. What's more, Dr. Flotch used Dual splitting method, gradient descent method and Incremental Stochastic Gradient Method as their optimization methods (5). These methods successfully address various aspects of PEV smart-charging and

also provide precise convergence analysis. This thesis also provided a comparison between the algorithms they provided. However, these methods are computationally expensive, as they may take a long time for computing when we use a complex data and systems. Previous work has studied various aspects of load shaping and PEV smart-charging including filling the night valley of loads (valley filling) in (6) (3), and grid constraints such as transformer overheating (7) (8),and local distribution grid constraints (9) (10) (11).

In this thesis, optimal charging strategies are added to existing studies on minimizing cost as follows. The Broyden–Fletcher–Goldfarb–Shanno (BFGS) algorithm in Quasi-Newton method is used as the optimization method. The reason I choose BFGS Quasi-Newton method instead of other optimization methods is because I learned BFGS algorithm from both optimization course and a statistic course during my graduate study. Compared to Newton's method, Quasi-Newton method has advantages of computationally cheap, and faster computation, and no need for deriving the second derivative. Instead, BFGS algorithm calculates a step by step approximated Hessian. While Newton's method use the second derivative to approximate the output, compared with Quasi-Newton method, Newton's method are more complicated in programming. However, disadvantages of Quasi-Newton method includes it requires more convergence steps than Newton's method. What's more, Quasi-Newton method has less precise convergence path than Newton's method.

In this thesis, the base voltage is calculated for each node at different time for two different grid system topologies. The first grid system is a traditional grid that consists of 18 charging stations. The second system is a micro-grid system that consists of 8 charging stations and 10 Distributed energy resources (DER) generations buses including fuel cell, micro-turbine and photovoltaic cell. Then two grid systems typologies are implemented using MATLAB, base voltage is calculated and objective functions were set up etc. Moreover, the existing optimization method is changed into BFGS Quasi-Newton method based on the MATLAB code provided

from (1).

The rest of the thesis is structured as follows: in section 2 the objective function and its constraints are described. The math in calculating the base voltage, and optimization methods is also described in section 2. Section 3 describes the topology of the two different grid systems. Section 3 also describes the power profiles, state of charge profiles, and voltage profiles of the PEV after using the optimization method. Section 4 interprets the optimization results and limitations and improvements for this thesis. Section 5 gives conclusion to this thesis.

2 EV Charging Optimization Method

In this section, we use the notation in Table 1 and develop an optimization problem for synthesizing PEV charging schedules.

Symbol	Description
c_k	cost of energy at each time step k
t	duration of time steps in hours
J	number of connected PEVs
K	amount of time steps of the connection time of each PEV
$w_k^i - s_k^i$	charging/discharging rate of each connected PEV i
p^i	nominal power of the charger of PEV i
$\overline{soc^i}$	upper constraints for the state of charge of PEV i
$\underline{soc^i}$	lower constraints for the state of charge of PEV i
soc_k^i	battery state of charge for PEV i at the end of time step k
soc_o^i	battery state of charge for PEV i before charging/discharging.
v_{min}	lower limit for charging/discharging rates of PEVs over voltage level
v_{max}	upper limit for charging/discharging rates of PEVs over voltage level
v_k^n	voltage level at node n of a grid with N nodes.
x_k^n	power reference for PEV at node n
V_{nom}	nominal voltage of the grid
h_k^n	current value for PEV connected to node n at time step k
l_k^n	active power for node n at time step k
R_k^n	resistance for a node n at time step k
$\tilde{A}_k$	conductance for each node n at time step k

Table 1: Captions and Labels.

2.1 Objective Function

The objective function is to minimize the cost of energy in charging PEVs. The objective function $\min_{w^i,s^i} \sum_{i=1}^{J} \sum_{k=1}^{K} c_k t(w_k^i - s_k^i)$ represents the minimum cost for charging and discharging total number of PEVs within time step k. We denote $w_k^i - s_k^i$ as the charging and discharging rate for a PEV.

$$\min_{w^i,s^i} \sum_{i=1}^{J} \sum_{k=1}^{K} c_k t(w_k^i - s_k^i) \tag{1}$$

where, parameters c represents the cost of energy at each time step k, and t represents the duration of time steps in hours, J is the number of connected PEVs,

and K is the amount of time steps of the connection time of each PEV. There are three type of constraints.

2.1.1 Constraints on Chargers

Firstly, constraints on the charger, Chargers are assumed to be able to handle bidirectional power flow. Moreover, distribution system substations may become overloaded and induce equipment failure and large power outages (12) (13). We consider preventing these dangerous side effects by setting active power capacity constraints. So they have limited rates of consumption/injection that must be taken into account in the load scheduling problem. Consumption and injection rates are limited by,

$$-p^i \leq x_k^i \leq p^i \tag{2}$$

where, p^i is the nominal power of the charger of a PEV labeled with index i.

2.1.2 Constraints on State of Charge

Secondly, constraints on partial and final steps of charge. To avoid impacting the batteries states of health due to deep discharging, partial state of charge must be constrained between certain boundaries.

$$\underline{soc^i} \leq soc_k^i \leq \overline{soc^i} \tag{3}$$

where, $\overline{soc^i}$ and $\underline{soc^i}$ are the upper and lower constraints for charging and discharging battery. For a PEV labeled i, the battery state of charge after time step k is:

$$soc_k^i = soc_o^i + t \sum_{K=1}^{k} (w_k^i - s_k^i) \tag{4}$$

$$\underline{soc^i} \leq soc_o^i + t \sum_{K=1}^{k} (w_k^i - s_k^i) \leq \overline{soc^i} \tag{5}$$

Reference (14) provides more details about setting up constraints to improve battery health.

2.1.3 Constraints on Voltage Levels

Thirdly, constraints on voltage levels, as the voltage levels are limited between a lower limit V_{min} and an upper limit V_{max}. And the voltages are non linear functions of variables like the instantaneous active and reactive powers.

$$v_{min} \leq v_k^n \leq v_{max} \tag{6}$$

where, v_k^n represents the voltage at node n of a grid with N nodes, at time step k.

2.2 Grid System

Load profiles for the 18-node grid system for every half hour are given, so the load for each node were divided into 48 values representing load values at every 30 minutes. When implementing the 18-node grid system into MATLAB, the load profile is a 18×48 matrix.

2.2.1 Calculating the Base Voltage

Given the load profile of the 18-node grid system at 48 different timeline, and their conductance coefficients, the plan is to calculate the base voltages for the 18-nodes at 48 different timelines. The following topology in Figure 1 represents currents flow in n nodes. v_k^{in} is the input voltage, R_{in}^n is the input resistance, R_{01}^n is the resistance for node 1, R_{02}^n is the input resistance for node 2, R_{0M}^n is the input resistance for node M, R_k^n is the resistance for node k, v_k^{01} is the voltage for node 1, v_k^{02} is the voltage for node 2, and v_k^{0M} is the voltage for node M.

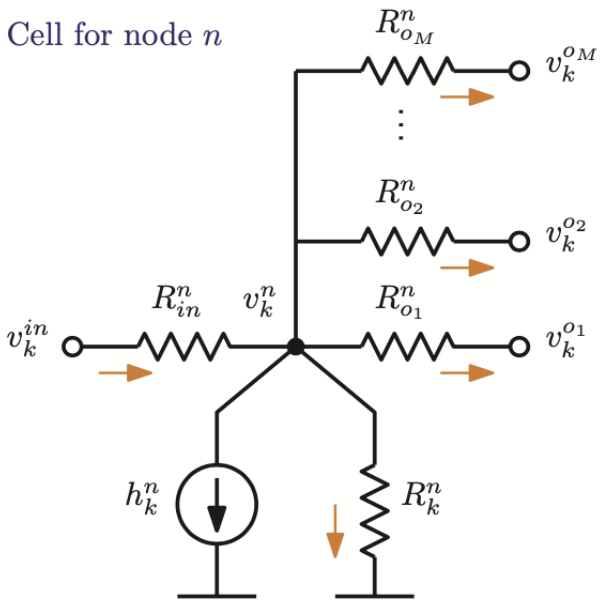

Figure 1: Currents flow in the approximated model of the grid.

By Kirchhoff's current law, currents can be represented as:

$$\begin{aligned} h_k^n = v_k^{in}\left(\frac{1}{R_{in}^n}\right) - v_k^n\left(\frac{1}{R_{in}^n} + \frac{1}{R_k^n} + \frac{1}{R_{01}^n} + \frac{1}{R_{02}^n} + \ldots + \frac{1}{R_{0M}^n}\right) \\ + v_k^{01}\frac{1}{R_{01}^n} + v_k^{02}\frac{1}{R_{02}^n} + \ldots + v_k^{0M}\frac{1}{R_{0M}^n} \end{aligned} \tag{7}$$

where, h_k^n is the current value for a PEV connected to node n at time step k.

$$h_k^n = \frac{x_k^n}{V_{nom}} \tag{8}$$

where, V_{nom} is the nominal voltage of the grid. x_k^n is the power reference for a PEV connected at node n. The resistance for a node at time k is:

$$R_k^n = \frac{V_{nom}^2}{l_k^n} \tag{9}$$

where, l_k^n is the active power for node n at time k. Organizing all the N equations for each node, we got:

$$\tilde{A}_k v_k = h_k + \frac{1}{R_0} v_k^0 \tag{10}$$

where, matrix $\tilde{A}_k$ collects all the conductance for each node at time k, and Matrix

$\tilde{A}_k$ is an 18 ×18 matrix. Plug in equation (7) into equation (9), we get:

$$\tilde{A}_k v_k = \frac{1}{V_{nom}} x_k + \frac{1}{R_0} v_k^0 \tag{11}$$

Defining A_k as the inverse matrix of $\tilde{A}_k$, the base voltage for each node at different time step k is:

$$v_k = \frac{1}{V_{nom}} A_k x_k + \frac{1}{R_0} A_k v_k^0 \tag{12}$$

The base voltage is an 18 × 48 matrix representing voltage for the 18 nodes at 48 different times. Reference (1) provides more details about how to calculate the base voltage.

2.3 Optimization Methods

Two optimization methods are used in this thesis. Quasi-newton methods has the advantages of computational cheapness, and usually requires less computation time. Furthermore, Quasi-Newton method doesn't need to compute the second derivative, while Newton's method needs to calculate the Hessian matrix. Moreover, Quasi-Newton method does not need to solve linear system of equations, but Newton's method needs to solve linear system of equations. There are also disadvantages about the Quasi-Newton method. Firstly, Quasi-Newton method usually requires more convergence steps, while Newton's method requires less convergence steps. Secondly, Quasi-Newton method has less precise convergence path, but Newton's method has more precise convergence path.

2.3.1 Newton's Method

Newton-Raphson method is a root-finding algorithm which produces successively better approximations to the roots (or zeroes) of a real-valued function. Newton's method starts with a function f for a variable x, the function's derivative f', and an initial guess of x_0 for a root of f.

$$x_1 = x_0 - \frac{f(x_0)}{f(x_0)'} \tag{13}$$

Where, x_1 is a better approximation of the root than x_0. (x_1,0) is the intersection between the x-axis and the tangent line for the graph of f at (x_0,$f(x_0)$): that is, the improved guess is the unique root of the linear approximation at the initial point. The process is repeated as:

$$x_{n+1} = x_n - \frac{f(x_n)}{f(x_n)'} \tag{14}$$

until a sufficiently precise value is reached.

2.3.2 Quasi-Newton Method

The Broyden-Fletcher-Goldfarb-Shanno algorithm (BFGS) is used in Quasi-Newton method. This algorithm determines the descent direction by preconditioning the gradient with curve information. BFGS does this by gradually improving an approximation to the Hessian matrix of the loss function. The first step is to find P_k from:

$$B_k P_k = -\nabla f(x_k) \tag{15}$$

where B_k is an approximation to the Hessian matrix. And it is updated each iteration. $\nabla f(X_k)$ is the gradient of the function evaluated at X_k. The next step is to do the line search using:

$$\alpha_k = argmin f(x_k + \alpha P_k) \tag{16}$$

A line search in the direction P_k is to find the next point X_{k+1}. The Quasi-Newton condition in updating B_k is:

$$B_{k+1}(x_{k+1} - x_k) = \nabla f(x_{k+1}) - \nabla f(x_k) \tag{17}$$

where $y_k = \nabla f(x_{k+1}) - \nabla f(x_k)$ and $s_k = \alpha_k P_k$, $x_{k+1} = x_k + s_k$. And finally the approximate Hessian B_{k+1}:

$$B_{k+1} = B_k + \frac{y_k y_k^T}{y_k^T s_k} - \frac{B_k s_k s_k^T B_k^T}{s_k^T B_k s_k} \tag{18}$$

3 Methodology

In this section the above methodology is adapted to include grid charging situation and grid capacity constraints, as studied in (1) (7) (15). This section explains the charging situation including how many PEVs start charging at a specific time under what electricity price. After explaining the charging situation, next section shows the input and output of the objective function used in MATLAB. And in scenario 1, this section used the first grid topology that contains 18 charging stations and then explains how the algorithm in Newton's method works, as well as how the algorithm in BFGS Quasi-Newton works. Then this section illustrates the optimization results obtained from the two methods. Next section shows scenario 2, the micro-grid topology that contains 8 charging stations and 10 Distributed Energy Resources (DER) generations node. and then explains the optimization result using both Newton's method and BFGS Quasi-Newton method.

3.1 Charging Situation

The model we assume is a dual tariff, nightly charging scheme. Dual tariff means the electricity has two different prices during different time intervals. While between 6AM to 10:59PM, the tariff for electricity price is 1.5 dollar per kWh, and between 11:00PM to 5:59 AM, the tariff for electricity price is 1 dollar per kWh (1). The reason that we have dual tariff electricity price is because households usually consume much more power in the daytime than in the night time. It offered us an easier way of optimizing costs by adjusting the times of higher electricity costs. We assume enough distribution capacities are available in the power grid. And the charger can handle bidirectional power flow which means that PEVs can charge electricity remaining in battery back to the charger during high tariff and starts to charge during the low tariff time.

Three PEVs are assumed to be charging in the grid. And PEV 1 is charging at node 3, PEV 2 is charge at node 8, and PEV 3 is charging at node 11. In order to

minimize the energy cost, the peak consumption should occur during the low tariff hours as the electricity price per KWh is lower, and during the high tariff hours, PEVs injects electricity inside their battery back to the charger to sell their initially stored energy. And at the same time keeping the voltage profiles correspond to each charging node within the desired limits. The battery capacity for the three PEVs is 20 kWh, but in order to protect the life span of the battery, we only charge to 80 percent of its full capacity which is 16 kWh.

3.2 Objective Function

The objective function has two outputs, '$powtrajast$' and 's'. '$powtrajast$' is the output that describes the optimal power trajectory, and 's' is the output that describes the max infeasibility bound on the voltage constraints.

```
function [pow_traj_ast,s] = ...
       Book_EV_Centralized_Scheduling_PhaseI(soc_c,soc_d,soc_0,p_max_c,...
       p_max_i,t_0,Ki,dt,A,v_0,v_k_base,v_max,v_min,Lhat,nodes,...
       watch_evolution)
```

Figure 2: Function that Minimizing the Bound on the Max in-feasibility of Voltage Constraints

The function aims to derive the bound "s" below zero in order to provide an initial guess for the charging schedules such that the voltage, state of charge, and power constraints are respected.

3.3 Scenario 1

In the topology subsection, a 35 nodes test grid system is considered. It is a 220V AC voltage grid with a voltage transformer at bus 2. In this grid system. There are eighteen power loads at each bus which include bus 4, 13, 14, 16, 17, 18, 20, 23, 24, 25, 27, 28, 29, two 31, 33, 34 and 35. The chargers in the 18 nodes can handle bi-direction power flow which means they be used in charging and discharging PEVs. And the system topology in Figure 3 shows below:

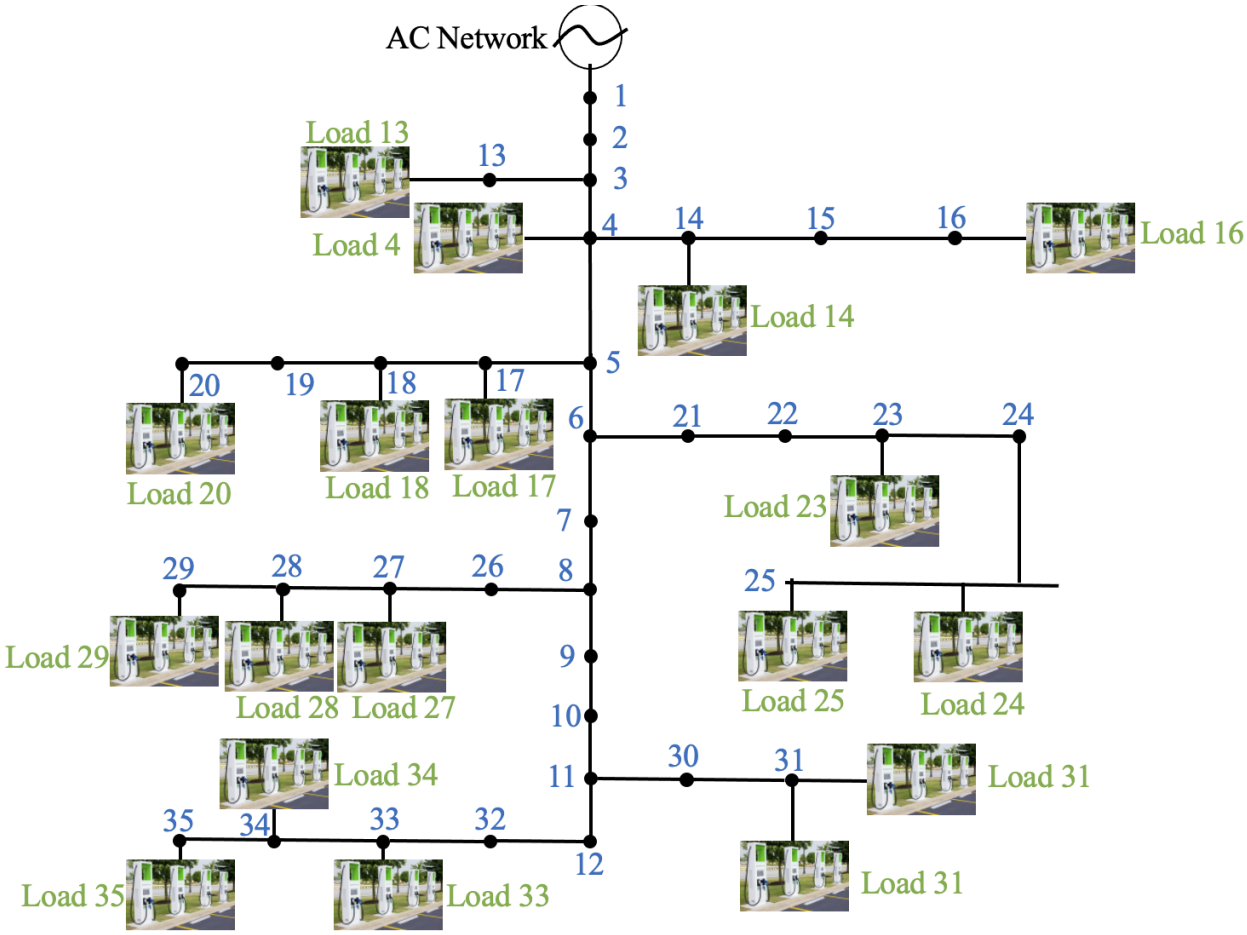

Figure 3: Grid System for Scenario 1

The system configuration for the grid system for line impedance between each buses is shown on Table 2. And the system configuration of the grid system for power loads at each bus is shown on Table 3.

From	To	$R(\Omega/km)$	$L(H/\text{km})$	Length(m)
3	4	0.2712	0.1856×10^{-3}	45
3	13	3.1200	0.2308×10^{-3}	50
4	14	3.1200	0.2308×10^{-3}	50
14	15	3.1200	0.2308×10^{-3}	50
15	16	3.1200	0.2308×10^{-3}	50
5	6	0.2712	0.1856×10^{-3}	45
17	18	2.4591	0.3256×10^{-3}	20
18	19	2.4591	0.3256×10^{-3}	20
19	20	2.4591	0.3256×10^{-3}	20
21	22	0.5260	0.3025×10^{-3}	30
22	23	0.5260	0.3025×10^{-3}	30
23	24	0.5260	0.3025×10^{-3}	30
24	25	0.5260	0.3025×10^{-3}	30
7	8	0.2712	0.1856×10^{-3}	45
26	27	0.7849	0.1906×10^{-3}	40
27	28	0.7849	0.1906×10^{-3}	40
28	29	0.7849	0.1906×10^{-3}	40
9	10	0.2712	0.1856×10^{-3}	45
10	11	0.2712	0.1856×10^{-3}	45
30	31	4.5600	0.3026×10^{-3}	30
11	12	0.2712	0.1856×10^{-3}	45
32	33	1.2613	0.1956×10^{-3}	30
33	34	1.2613	0.1956×10^{-3}	30
34	35	1.2613	0.1956×10^{-3}	30

Table 2: Line impedance between buses

3.3.1 Newton's Method

Then Newton's method starts with a loop with iteration index one, and initializes s with a starting value. Then computes the objective function's current value, and after that computes the gradient of the extended objective function. Then computes the Hessian of the objective function. Next step is to compute the direction of descent using backtracking line search. Update values of s and stop when the decrement is less than the threshold. The algorithm 1 shows as follows.

Bus	P_n(kW)	Q_n(kVAR)
4	32.69	15.97
14	74.69	41.26
17	41.56	27.64
23	59.63	38.57
25	60.54	40.63
28	61.35	37.59
31	58.21	36.78
33	65.31	39.45
13	5.36	3.65
16	15.36	10.25
18	20.00	15.25
20	10.25	5.68
25	64.59	54.26
27	25.69	15.75
29	25.00	12.00
31	45.30	30.65
34	36.78	14.23
35	29.24	14.96

Table 3: Power loads at each bus

Algorithm 1: Newton's Method
Initializations: max infeasibility bound on voltage constraints
for $n = 1$ to N
compute the states of charge trajectories and voltage contribution of PEVs
compute objective function's current value
compute the gradient of the objective function
compute the Hessian of the objective function
compute the direction of descent
backtracking line search
if stopping criteria are reached then stop
end for loop
update the output

Applying the proposed PEV load management approach using Newton's method into the two tariff scenarios. The results are divided into four subplots. Newton's method used 81 iterations to get the results, The results for Newton's method are as follows in Figure 4:

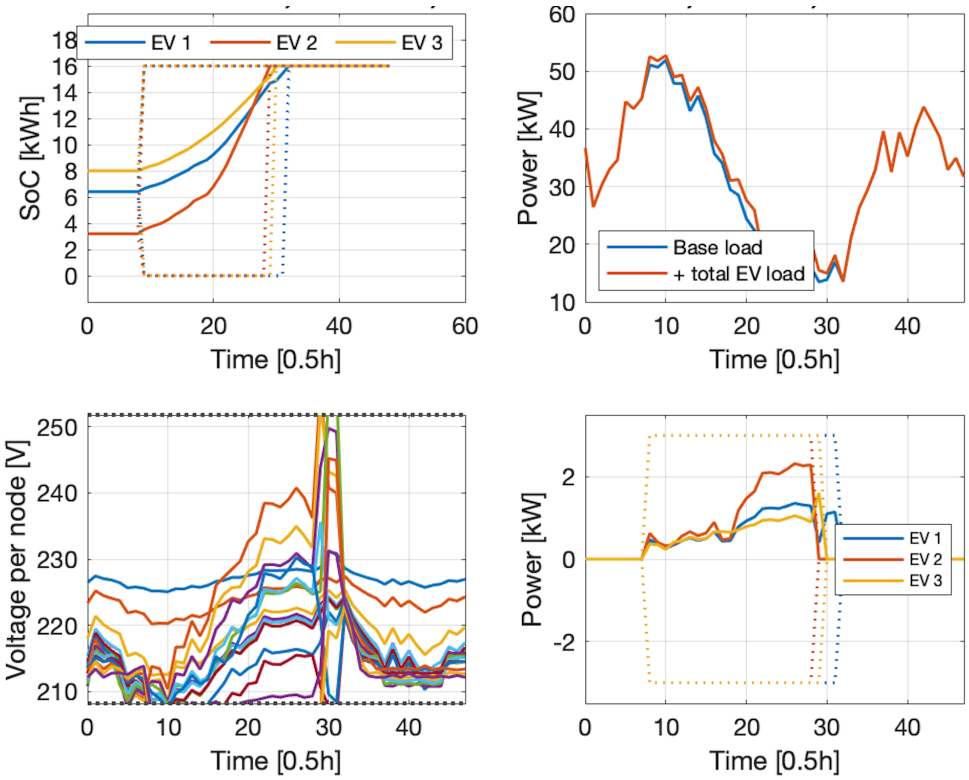

Figure 4: Results for Newton's Method

From subplot 1, blue line represents the first PEV, red line represents the second PEV, and yellow line represents the third PEV. The horizontal axis is the time in every half hour. And the vertical axis is the state of charge of the battery for the three PEVs. We can see that all the three PEVs are charging their battery at the low tariff hours until they fully charge their battery. The dotted line shows the upper limit and lower limit for state of charge. As Figure 5 shows:

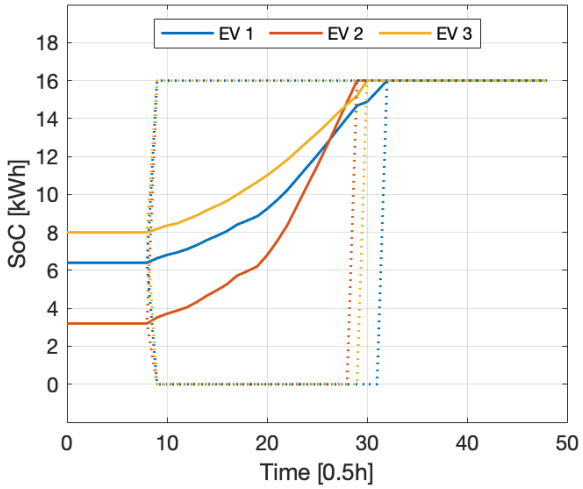

Figure 5: State of Charge Subplots Using Newton's Method

From subplot 2, the blue line represents the total base load for the 18 nodes. And the red line represents the the total base load plus the total three EV loads. We can see that during the time from 20-30, the total EV loads is using significantly more than the base load. As Figure 6 shows:

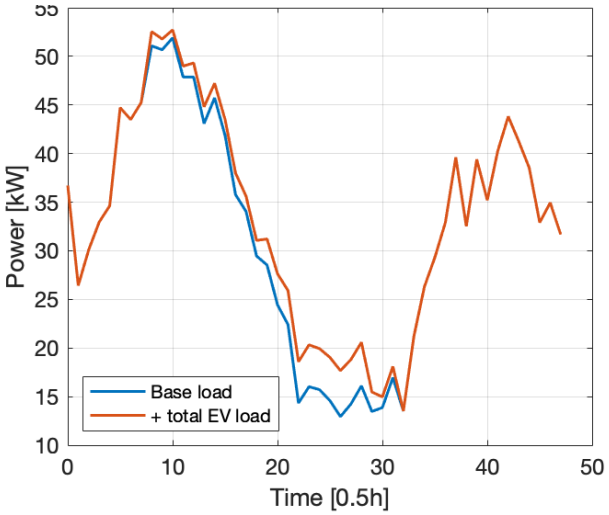

Figure 6: Total Load Subplots Using Newton's Method

From subplot 3, it shows the load profiles for the 18 nodes at different time zones. The dotted line shows the upper voltage limit and lower voltage limit. We can see that they are stayed within the upper voltage limit 260 volts and lower voltage limit 200 volt. As Figure 7 shows:

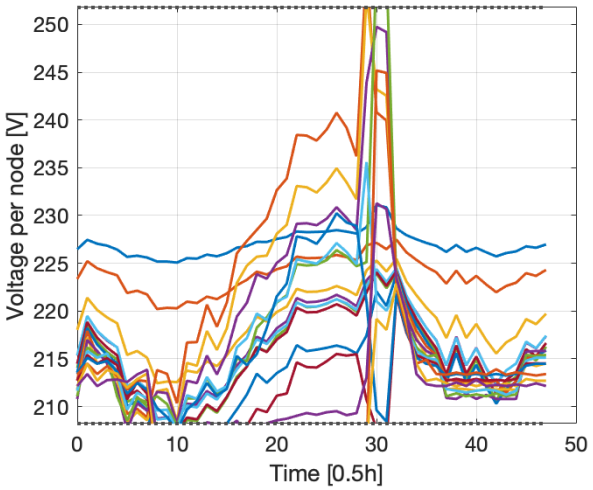

Figure 7: Voltage Per Node Subplot Using Newton's Method

From subplot 4, it shows the power for each EV. Blue line represents the first EV, and red line represents the second EV, and yellow line represents the third EV. The

dotted line shows the upper power limit and lower power limit for each PEV. All power of the three EV stayed within the upper limit 3kW and lower limit -3 kW. As Figure 8 shows:

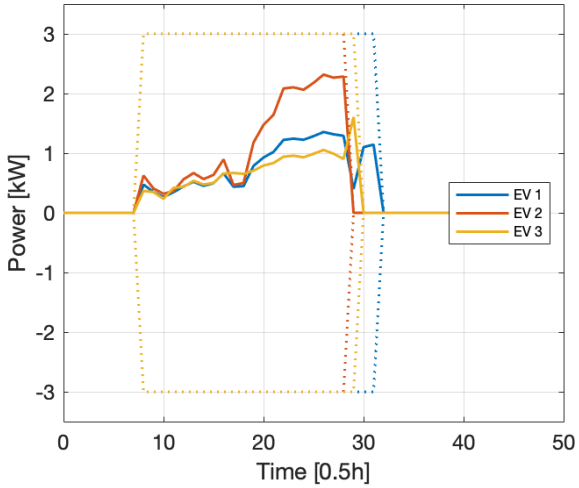

Figure 8: EV Power Subplot Using Newton's Method

Based on the above, the three PEVs didn't sell their initially stored energy. So the cost of charging is not optimized.

3.3.2 BFGS Quasi-Newton Method

The Quasi-Newton method starts with a for loop with iteration index 1 and initializes s, the max infeasibility bound on the voltage constraints. And initialize B_k into an identity matrix with length same as the gradient of the extended objective function. Let y_k equals to the gradient of the objective function minus the initialized y. And approximate the Hessian B_{k+1} as following in Figure 9:

```
if ii==1
    B_k=eye(length(dH_dus));
    y = dH_dus;
else
    Delta_y = dH_dus-y;
    y=dH_dus;
    delta_Bk = (Delta_y*Delta_y')/(Delta_y'*Delta_x)-(B_k*Delta_x*Delta_x'*B_k)/(Delta_x'*B_k*Delta_x);
    B_k = B_k+delta_Bk;
end
Hessian = B_k;
```

Figure 9: BFGS Approximation in MATLAB

And the algorithm 2 for BFGS method shows as follows:

Algorithm 2: BFGS Quasi-Newton's Method
Initializations: max infeasibility bound on voltage constraints
for $n = 1$ to N
compute the states of charge trajectories and voltage contribution of EVs
compute objective function's current value
compute the gradient of the objective function
compute the approximate Hessian of the objective function
compute the direction of descent
backtracking line search
if stopping criteria are reached then stop
end for loop
update the output

Applying the proposed PEV load management approach using BFGS Quasi-Newton's method into the two tariff scenarios. The results are divided into four subplots. BFGS Quasi-Newton's method used 420 iterations to get the results, The results for Newton's method are as follows in Figure 10:

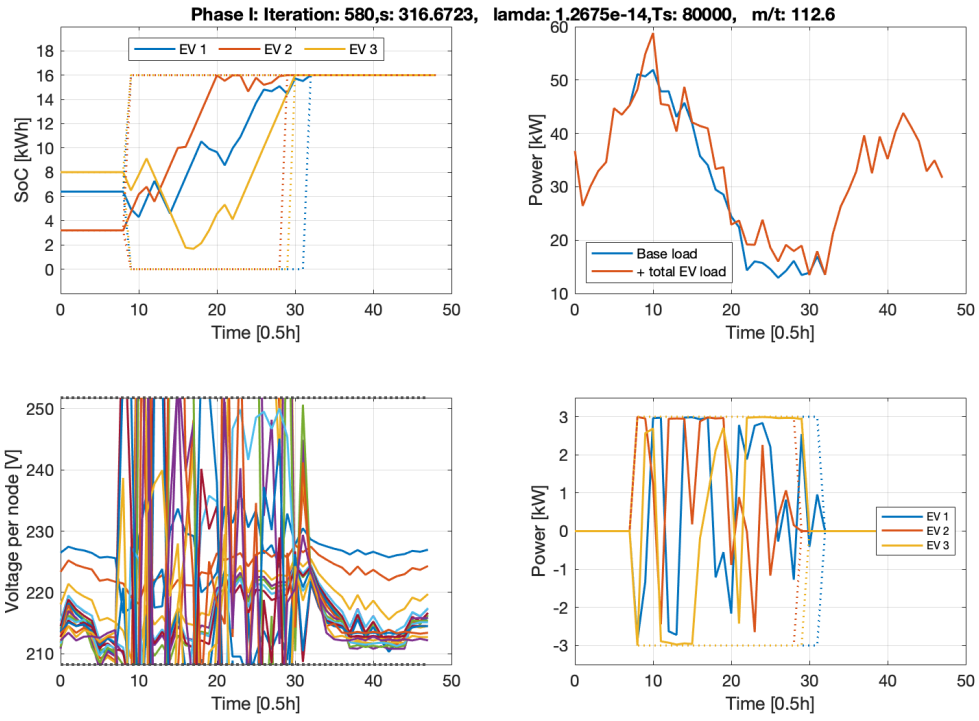

Figure 10: Results for BFGS Quasi-Newton's Method

From subplot 1, blue line represents the first PEV, red line represents the second PEV, and yellow line represents the third PEV. The horizontal axis is the time in every half hour. And the vertical axis is the state of charge of the battery for the

three PEVs. We can see that the first and the second PEVs are selling their initially stored energy when the tariff is high, and during the low tariff hours, all the three PEVs start charging their battery until they fully charge their battery. The dotted line shows the upper limit and lower limit for state of charge. As Figure 11 shows:

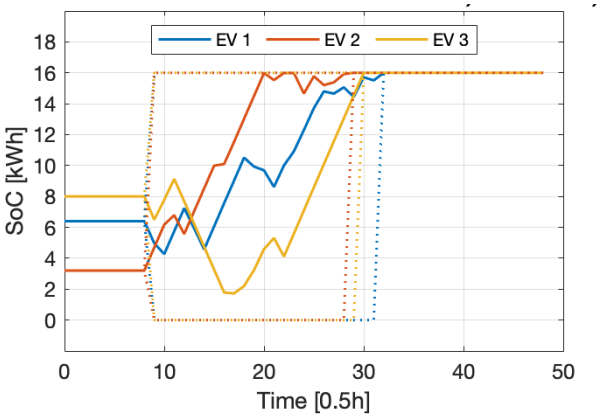

Figure 11: State of Charge Subplots Using BFGS Quasi-Newton's Method

From subplot 2, the blue line represents the total base load for the 18 nodes. And the red line represents the the total base load plus the total three EV loads. We can see that during the time from 20-30, the total EV load is using significantly more than the base load. As Figure 12 shows:

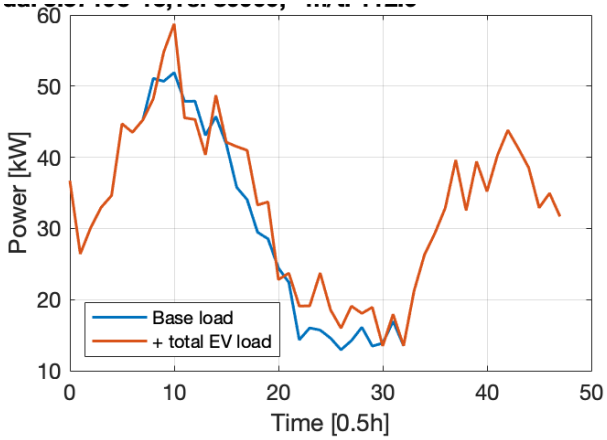

Figure 12: Total Load Subplots Using Quasi-Newton's Method

From subplot 3, it shows the load profile for the 18 nodes at different time zones. The dotted line shows the upper voltage limit and lower voltage limit. We can see

that during time from 10 to 30, voltage for nodes are not staying within the upper voltage limit 260 volts and lower voltage limit 200 volt, and the voltages for different nodes are fluctuating significantly during time from 10 to 30. As Figure 13 shows:

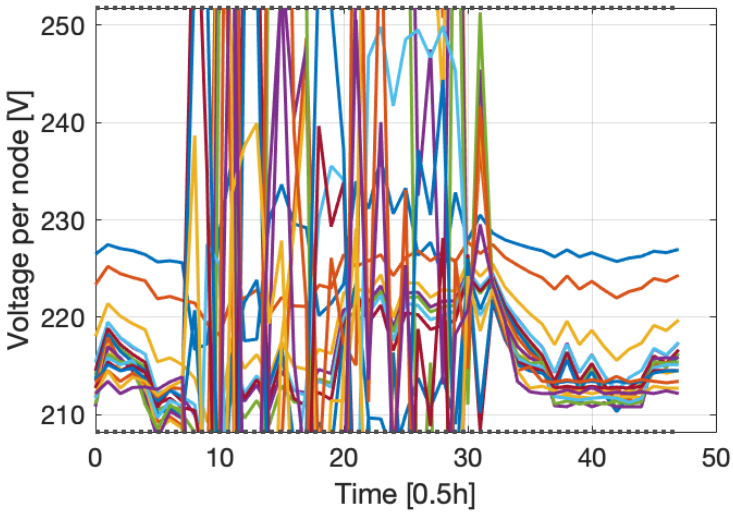

Figure 13: Voltage Per Node Subplot Using Quasi-Newton's Method

From subplot 4, it shows the power for each PEV. The blue line represents the first PEV, and the red line represents the second PEV, and the yellow line represents the third PEV. The dotted line shows the upper power limit and lower power limit for each PEV. All powers of the three PEVs stayed within the upper limit 3kW and lower limit -3 kW. The power for the three PEVs using BFGS Quasi-Newton Method are fluctuating more than the powers for the three PEVs using Newton's method. As Figure 14 shows:
Based on the state of charge subplot, the first and the third PEVs are selling their initially stored energy back to the charger, so the cost of charging is reduced. And the power and voltage for the nodes are kept within lower and upper limits.

3.4 Scenario 2

In the topology subsection, a 35 nodes test micro-grid system is considered. It is a 220V AC voltage grid with a voltage transformer at bus 2. In this grid system, there are four photo-voltaic at bus 16, 18, 29, and 35. There are eight power loads at each bus which include bus 4, 14, 17, 23, 25, 28, 31, and 33. In this test micro-grid system, there are ten Distributed Energy Resources (DER) generations buses which are 13,

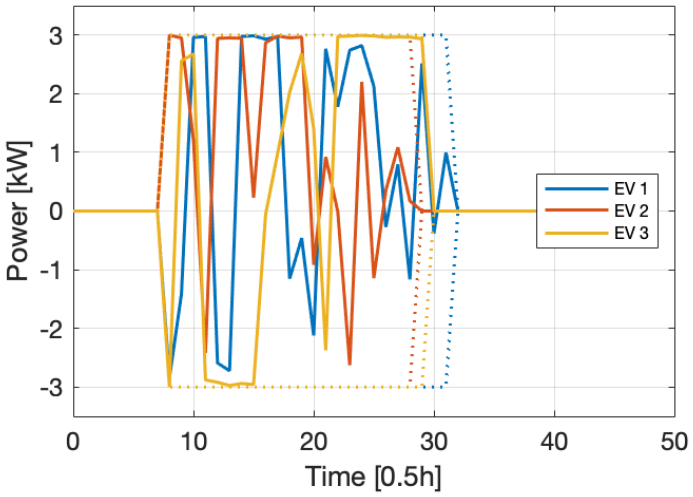

Figure 14: EV Power Subplot Using Quasi-Newton's Method

16, 18, 20, 25, 27, 29, 31, 34, and 35. While only 18 nodes can be used in charging and discharging PEVs because there are 8 power loads plus 10 Distributed Energy Resources (DER) generation buses in total. DER generation is electrical generation and storage performed by a variety of small, grid-connected or distribution system-connected devices. The system topology in figure 15 shows below:

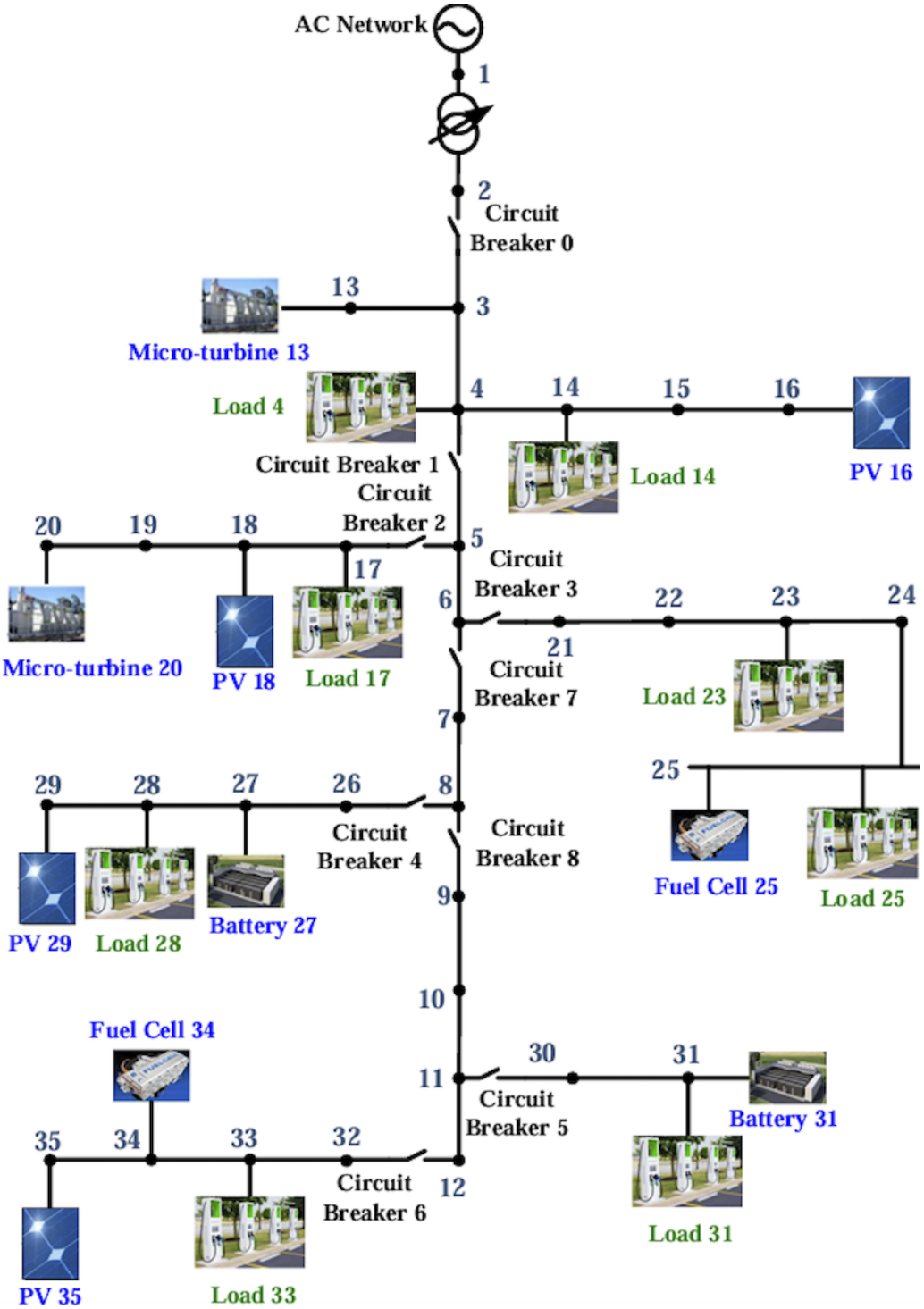

Figure 15: Micro Grid System for Scenario 2

The system configuration for the grid system for line impedance between each buses is given in table 2 in Scenario 1.

And the system configuration of the grid system for power loads at each bus is shown on Table 4 below:

Bus	P_n(kW)	Q_n(kVAR)
4	32.69	15.97
14	74.69	41.26
17	41.56	27.64
23	59.63	38.57
25	60.54	40.63
28	61.35	37.59
31	58.21	36.78
33	65.31	39.45

Table 4: Power loads at each bus

The system configurations of the grid system for DER generations at each bus is shown on Table 5 below:

Bus	P_n(kW)	Q_n(kVAR)
13	5.36	3.65
16	15.36	10.25
18	20.00	15.25
20	10.25	5.68
25	64.59	54.26
27	25.69	15.75
29	25.00	12.00
31	45.30	30.65
34	36.78	14.23
35	29.24	14.96

Table 5: DER generations at each bus

In the load profile, the loads are changed into negative values for the ten DER generation nodes. And the other eight power nodes have positive load values.

3.4.1 Newton's Method

Applying the proposed PEV load management approach using Newton's method into the two tariff scenarios. The results are divided into four subplots. Newton's method used 78 iterations to get the results, The results for Newton's method are as follows in Figure 15:

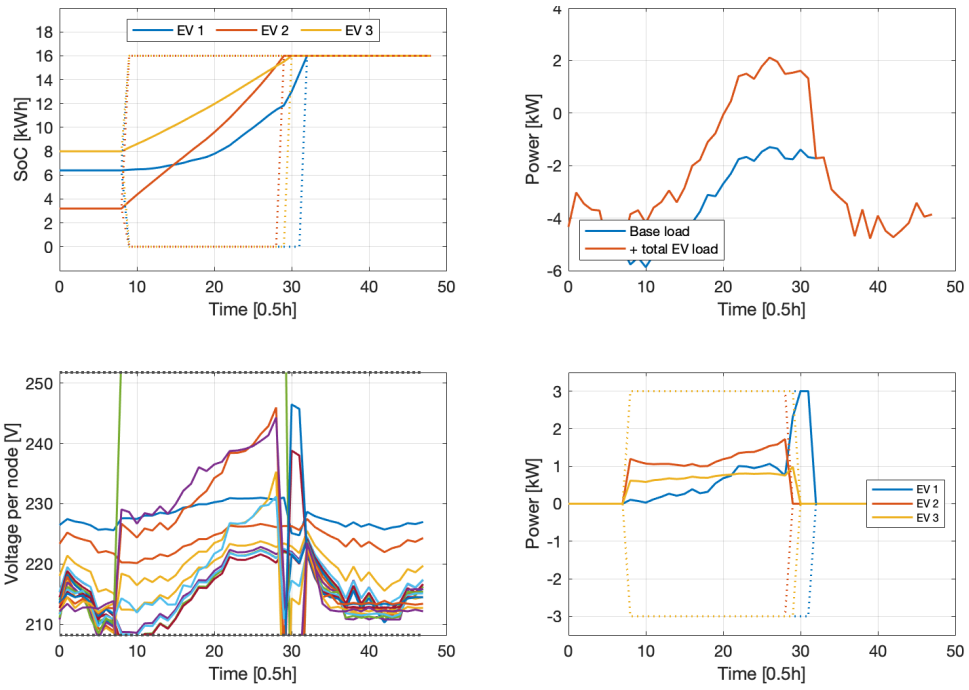

Figure 16: Results for Newton's Method for Scenario 2

From subplot 1, blue line represents the first PEV, red line represents the second PEV, and yellow line represents the third PEV. The horizontal axis is the time in every half hour. And the vertical axis is the state of charge of the battery for the three PEVs. We can see that the second PEV is charging with a constant speed, and it's charging faster than the other two PEVs as the slope for the red line is steeper than the other two lines. The first PEV is charging with the slowest speed, but it starts charging with a very fast speed at the low tariff hours. The dotted line shows the upper limit and lower limit for state of charge. As Figure 17 shows:

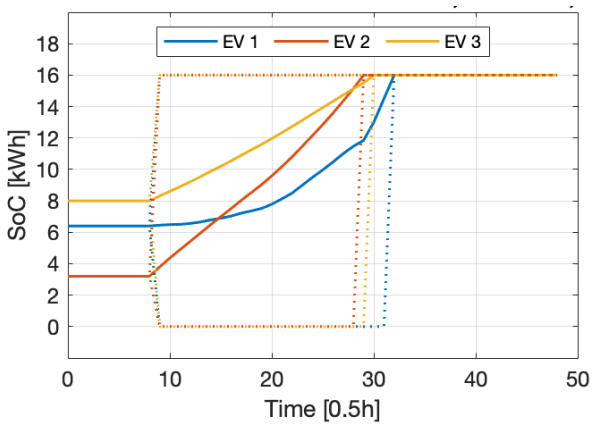

Figure 17: Results for State of Charge Subplots Using Newton's Method for Scenario 2

From subplot 2, the blue line represents the total base load for the 18 nodes. And the red line represents the the total base load plus the total three EV loads. The power for the base load is negative, which is caused by DER generation buses produced power back to the grid system. We can see that during the time from 10-30, the total EV load is using significantly more than the base load. This is because the charging of EV consumes a great amount of power from the time interval 10 to 30. As Figure 18 shows:

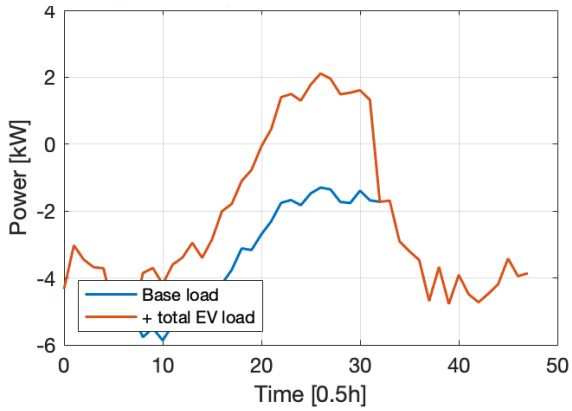

Figure 18: Total Load Subplots Using Newton's Method for Scenario 2

From subplot 3, it shows the load profiles for the 18 nodes at different time zones. The dotted line shows the upper voltage limit and lower voltage limit. We can see that they stayed within the upper voltage limit 260 volts and lower voltage limit 200 volt. The node representing in green line reached the 260 volts. As Figure 19 shows:

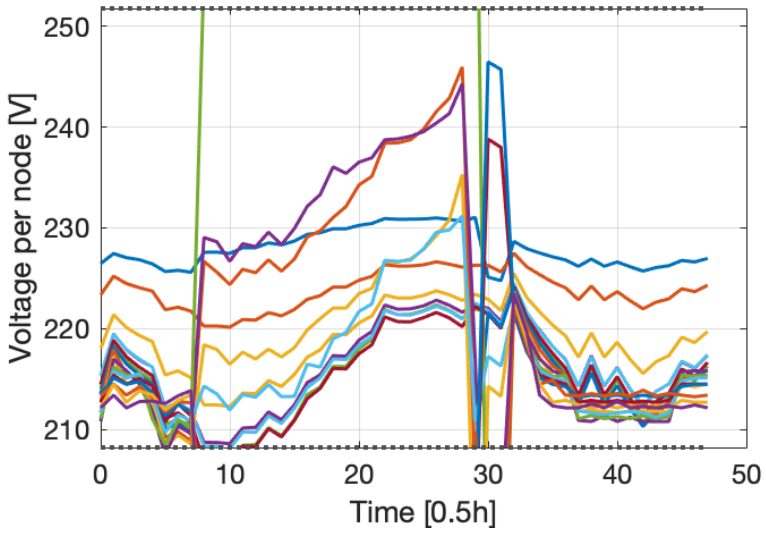

Figure 19: Voltage Per Node Subplot Using Newton's Method for Scenario 2

From subplot 4, it shows the power for each PEV. The blue line represents the first PEV, and the red line represents the second PEV, and the yellow line represents the third PEV. The dotted line shows the upper power limit and lower power limit for each PEV. All powers of the three PEV stayed within the upper limit 3kW and lower limit -3 kW. The power of the first PEV rising significantly from the time interval between 28 to 30. Because the first PEV starts charging during this time interval so it consumes a large amount of power. As Figure 20 shows:

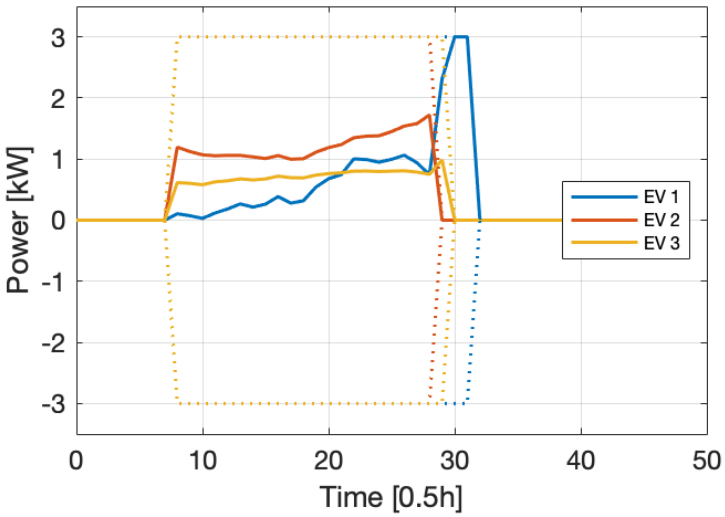

Figure 20: EV Power Subplot Using Newton's Method for Scenario2

3.4.2 BFGS Quasi-Newton Method

Applying the proposed PEV load management approach using BFGS Quasi-Newton's method to the two tariff scenarios. The results are divided into four subplots. BFGS Quasi-Newton's method used 310 iterations to get the results, The results for Newton's method are as follows in Figure 21:

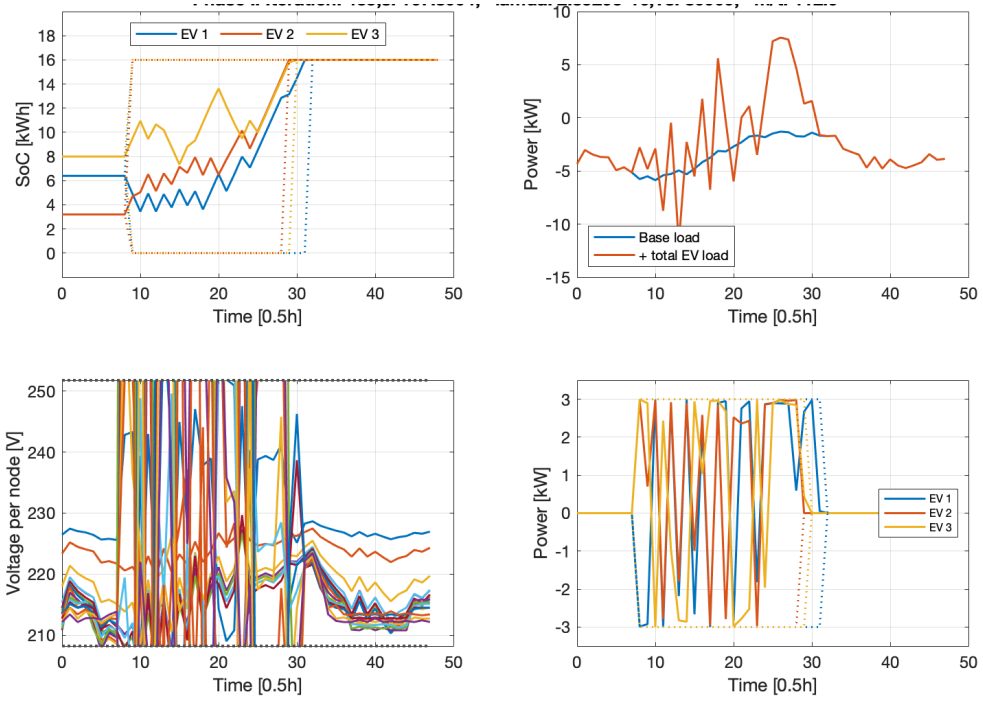

Figure 21: Results for BFGS Quasi-Newton's Method for Scenario 2

From subplot 1, the blue line represents the first PEV, the red line represents the second PEV, and the yellow line represents the third EV. The horizontal axis is the time in every half hour. And the vertical axis is the state of charge of the battery for the three PEVs. At first, we can see that the first PEV in blue line is selling its initially stored energy into the grids while the other two PEVs are not selling its energy back to the grid at beginning. All the three PEVs increased their charging speed at the low tariff hour until they fully charge their battery. The dotted line shows the upper state of charge limit and lower state of charge limit. As Figure 22 shows:

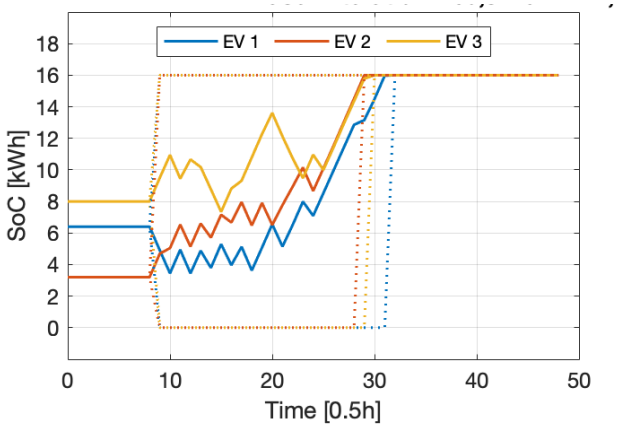

Figure 22: State of Charge Subplots Using Quasi-Newton's Method for Scenario 2

From subplot 2, the blue line represents the total base load for the 18 nodes. And the red line represents the the total base load plus the total three PEV loads. The power for the base load is negative, which is caused by DER generation buses produced power back to the grid system. We can see that during the time from 20-30, the total PEV load is using more than the base load. And the usage of total load in charging PEV has rising significantly during the time interval between 25-30. As Figure 23 shows:

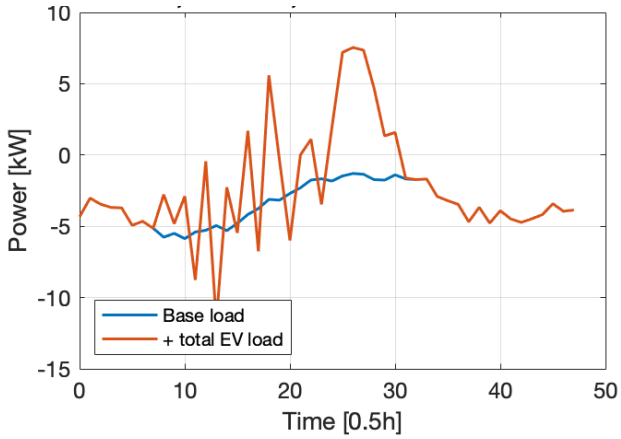

Figure 23: Total Load Subplots Using Quasi-Newton's Method for Scenario 2

From subplot 3, it shows the load profiles for the 18 nodes at different time zones. The dotted line shows the upper voltage limit and lower voltage limit. We can see that from 10 to 30, voltage for nodes exceeded the upper voltage limit 260 volts and lower voltage limit 200 volt, and the voltages for different nodes are fluctuating significantly during time from 10 to 30. As Figure 24 shows:

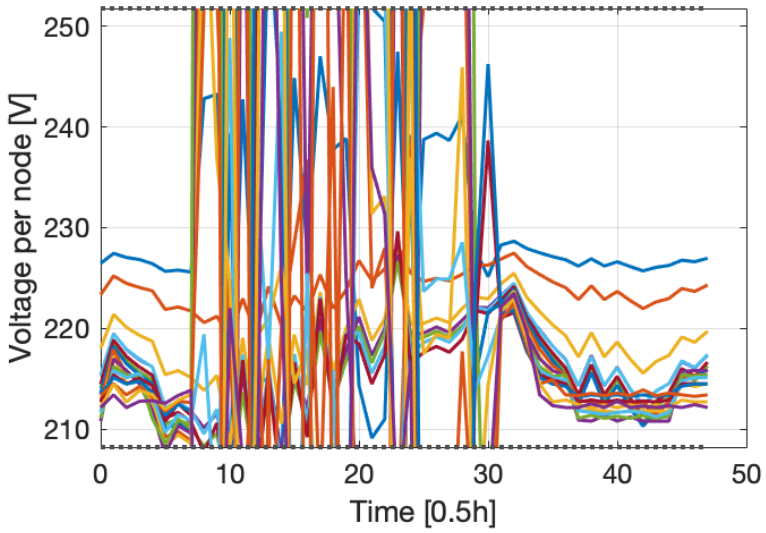

Figure 24: Voltage Per Node Subplot Using Quasi-Newton's Method for Scenario 2

From subplot 4, it shows the power for each PEV. The blue line represents the first PEV, and the red line represents the second PEV, and the yellow line represents the third PEV. The dotted line shows the upper power limit and lower power limit for each PEV. All powers of the three PEVs stayed within the upper limit 3kW and lower limit -3 kW. The power for the three PEVs using BFGS Quasi-Newton Method are fluctuating more than the powers for the three PEVs using Newton's method. As Figure 25 shows:

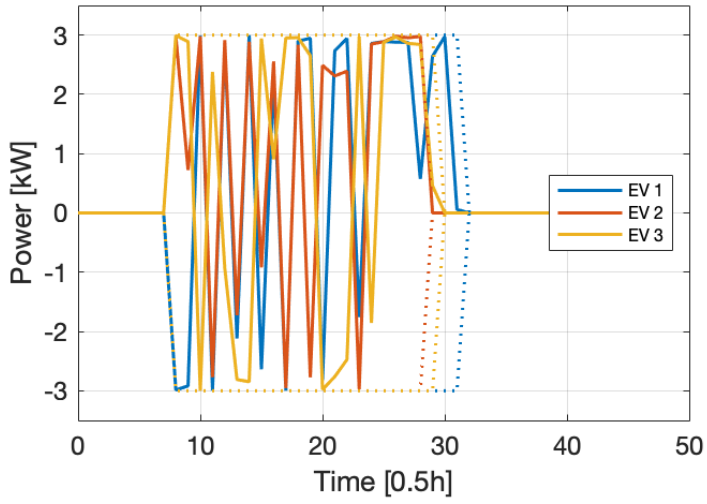

Figure 25: EV Power Subplot Using Quasi-Newton's Method for Scenario 2

4 Discussion

4.1 Comparison Between Newton's method and BFGS Quasi-Newton Method

Based on the plots from result section that shows PEV power and the state of charge, in both Scenario 1 and Scenario 2, three PEVs are not selling their initially stored energy back to the chargers at the high tariff hour using Newton's method. However, the three PEVs are selling their initially stored energy back to the chargers when using BFGS Quasi-Newton method. Therefore, the cost of charging is lower for using BFGS Quasi-Newton method. However, the plot for voltage per node is steady using Newton's method, while the plot for voltage per node fluctuates a lot when using BFGS Quasi-Newton method. Comparing the total node power plots between grid system in scenario 1 and scenario 2, the base load in scenario 2 is negative, which is caused by DER generation buses produced power back to the grid system. And the total amount of power that produced exceeds the total power consumption of charging the three PEVs.

4.2 Limitations and Improvements

There are still many improvements in using the BFGS Quasi-Newton method. It used 420 iterations to get the approximate Hessian and end the loop. Results using BFGS Quasi-Newton method used more iterations when compared to the Newton's method, as Newton's method only used 81 iterations to get the optimizing result. Moreover, the results using Quasi-Newton method has too many fluctuations. The result may get over optimized. Furthermore, in voltage per node subplot, during time 10 to 30, voltages for nodes exceeded the upper voltage limit and lower voltage limits.

Limitations to this thesis also include failed to calculate the exact value of charging price for both scenario 1 and scenario 2. I will solve this problem in future work.

So improvement that will be explored in the future includes change the stopping criteria in coding for the BFGS Quasi-Newton method to reduce the fluctuations in state of charge plot and power plot.

More future improvement can include adding constraints for node voltages when using BFGS Quasi-Newton method, and keep the node voltages within the upper voltage limit and lower voltage limit.

5 Conclusion

This thesis aims to minimize the cost for charging PEVs using BFGS Quasi-Newton method. We defined the objective function, and set up constraints relate to state of charge, charging power, charging voltage, and calculated the base voltage using Kirchhoff's circuit law. Then in the next section, we implemented the optimization algorithms for two different grid systems. The first grid system is an 18 power nodes charging system, and the second one is a micro-grid system that consists of 8 power node and 10 DER generation nodes. Then we illustrated the result using state of charge subplot, power plot for nodes, voltage plot for different nodes, and total power for charging PEVs. And then compared the result with Newton's method.

Finally, we showed that BFGS Quasi-Newton method is also a good optimization method that can be used to minimize the cost for charging PEVs, and the result shows it has a lower cost in charging PEVs than using Newton's method in same grid topology and same situation.

References

[1] A. Ovalle, A. Hably, and S. Bacha, "Optimal management and integration of electric vehicles to the grid: Dynamic programming and game theory approach," in *2015 IEEE International Conference on Industrial Technology (ICIT)*, 2015, pp. 2673–2679.

[2] O. Sundström and C. Binding, "Optimization methods to plan the charging of electric vehicle fleets," in *Proceedings of the international conference on control, communication and power engineering*. Citeseer, 2010, pp. 28–29.

[3] L. Gan, U. Topcu, and S. H. Low, "Optimal decentralized protocol for electric vehicle charging," *IEEE Transactions on Power Systems*, vol. 28, no. 2, pp. 940–951, 2012.

[4] A. Langton and N. Crisostomo, "Vehicle-grid integration: A vision for zero-emission transportation interconnected throughout california's electricity system," *California Public Utilities Commission, Tech. Rep*, vol. 13, 2013.

[5] C. Le Floch, F. Belletti, and S. Moura, "Optimal charging of electric vehicles for load shaping: A dual-splitting framework with explicit convergence bounds," *IEEE Transactions on Transportation Electrification*, vol. 2, no. 2, pp. 190–199, 2016.

[6] Z. Ma, D. S. Callaway, and I. A. Hiskens, "Decentralized charging control of large populations of plug-in electric vehicles," *IEEE Transactions on control systems technology*, vol. 21, no. 1, pp. 67–78, 2011.

[7] S. Shao, M. Pipattanasomporn, and S. Rahman, "Demand response as a load shaping tool in an intelligent grid with electric vehicles," *IEEE Transactions on Smart Grid*, vol. 2, no. 4, pp. 624–631, 2011.

[8] S. Vandael, N. Boucké, T. Holvoet, and G. Deconinck, "Decentralized demand side management of plug-in hybrid vehicles in a smart grid," in *Proceedings of the first international workshop on agent technologies for energy systems (ATES 2010)*, 2010, pp. 67–74.

[9] N. Chen, C. W. Tan, and T. Q. Quek, "Electric vehicle charging in smart grid: Optimality and valley-filling algorithms," *IEEE Journal of Selected Topics in Signal Processing*, vol. 8, no. 6, pp. 1073–1083, 2014.

[10] O. Sundstrom and C. Binding, "Flexible charging optimization for electric vehicles considering distribution grid constraints," *IEEE Transactions on Smart grid*, vol. 3, no. 1, pp. 26–37, 2011.

[11] W.-J. Ma, V. Gupta, and U. Topcu, "On distributed charging control of electric vehicles with power network capacity constraints," in *2014 American Control Conference*. IEEE, 2014, pp. 4306–4311.

[12] J. Taylor, A. Maitra, M. Alexander, D. Brooks, and M. Duvall, "Evaluations of plug-in electric vehicle distribution system impacts," in *IEEE PES General Meeting*. IEEE, 2010, pp. 1–6.

[13] M. Kintner-Meyer, K. Schneider, and R. Pratt, "Impacts assessment of plug-in hybrid vehicles on electric utilities and regional us power grids, part 1: Technical analysis," *Pacific Northwest National Laboratory*, vol. 1, pp. 1–20, 2007.

[14] S. J. Moura, J. L. Stein, and H. K. Fathy, "Battery-health conscious power management in plug-in hybrid electric vehicles via electrochemical modeling and stochastic control," *IEEE Transactions on Control Systems Technology*, vol. 21, no. 3, pp. 679–694, 2012.

[15] L. Gan, U. Topcu, and S. H. Low, "Stochastic distributed protocol for electric vehicle charging with discrete charging rate," in *2012 IEEE Power and Energy Society General Meeting*. IEEE, 2012, pp. 1–8.